Shape Reconstruction of Inverse Medium Scattering for the Helmholtz Equation

Gang Bao* and Peijun Li†

Abstract

Consider a time-harmonic electromagnetic plane wave incident on a medium enclosed by a bounded domain in two dimensions. In this paper, existence and uniqueness of the variational problem for direct scattering are established. An energy estimate for the scattered field is obtained on which the Born approximation is based. Fréchet differentiability of the scattering map is examined. A continuation method for the inverse obstacle scattering problem, which reconstructs the shape of the inhomogeneous mediums from boundary measurements of the scattered wave, is developed. The algorithm requires multi-frequency data. Using an initial guess from the Born approximation, each update of the shape, represented by the level set function, is obtained via recursive linearization on the wavenumber by solving one forward problem and one adjoint problem of the Helmholtz equation.

Key Words. inverse obstacle scattering, shape reconstruction, Helmholtz equation, recursive linearization, level set function

AMS subject classifications. 65N21, 78A46

1 Introduction

Consider the Helmholtz equation in two dimensions

$$\Delta\psi^{\rm tot} + \kappa^2\varepsilon\psi^{\rm tot} = 0, \tag{1.1}$$

where $\psi^{\rm tot}$ is the total electric field, $\kappa > 0$ is the wavenumber, and ε is the relative electric permittivity. Rewrite $\varepsilon = 1 + q(\mathbf{x})$ and $q(\mathbf{x}) > -1$, which has a compact support, is the scatterer.

The total electric field $\psi^{\rm tot}$ consists of the incident field $\psi^{\rm inc}$ and the scattered field ψ:

$$\psi^{\rm tot} = \psi^{\rm inc} + \psi.$$

Assume that the incident field is a plane wave

$$\psi^{\rm inc}(\mathbf{x}) = e^{{\rm i}\kappa\mathbf{x}\cdot\mathbf{d}}, \tag{1.2}$$

*Department of Mathematics, Zhejiang University, Hangzhou 310027, China; Department of Mathematics, Michigan State University, East Lansing, MI 48824 (bao@math.msu.edu). The research was supported in part by the NSF grants DMS-0604790, DMS-0908325, CCF-0830161, EAR-0724527, and DMS-0968360, and the ONR grant N00014-09-1-0384, and a special research grant from Zhejiang University.

†Department of Mathematics, Purdue University, West Lafayette, IN 47907 (lipeijun@math.purdue.edu). The research was supported in part by the NSF grants DMS-0914595 and DMS-1042958.

where $\mathbf{d} \in \mathbb{S}^1 = \{\mathbf{x} \in \mathbb{R}^2 : |\mathbf{x}| = 1\}$ is the propagation direction. Evidently, such an incident wave satisfies the homogenous equation

$$\Delta\psi^{\rm inc} + \kappa^2\psi^{\rm inc} = 0. \tag{1.3}$$

It follows from the equations (1.1) and (1.3) that the scattered field satisfies

$$\Delta\psi + \kappa^2(1+q)\psi = -\kappa^2 q\psi^{\rm inc}. \tag{1.4}$$

In addition, the scattered field is required to satisfy the following Sommerfeld radiation condition

$$\lim_{\rho\to\infty} \sqrt{\rho}\left(\frac{\partial\psi}{\partial\rho} - {\rm i}\kappa\psi\right) = 0, \quad \rho = |\mathbf{x}|,$$

uniformly along all directions $\mathbf{x}/|\mathbf{x}|$. In practice, it is convenient to reduce the problem to a bounded domain by introducing an artificial surface. Let Ω be the compact support of the scatterer $q(\mathbf{x})$. Assume that $R > 0$ is a constant, such that the support of the scatterer, Ω, is included in the open ball $B = \{\mathbf{x} \in \mathbb{R}^2 : |\mathbf{x}| < R\}$. Let S be the sphere of the ball, i.e., $S = \{\mathbf{x} \in \mathbb{R}^2 : |\mathbf{x}| = R\}$. Denote $\mathbf{n}$ the outward unit normal to S. A suitable boundary condition then has to be imposed on S. For simplicity, we employ the first order absorbing boundary condition [16] as

$$\partial_{\mathbf{n}}\psi - {\rm i}\kappa\psi = 0, \quad \text{on } S. \tag{1.5}$$

Given the incident field $\psi^{\rm inc}$, the direct scattering problem is to determine the scattered field ψ for the known scatterer q. Based on the Lax–Milgram lemma, the direct problem is shown to have a unique solution for all but possibly a discrete set of wavenumbers. Furthermore, an energy estimate for the scattered filed, with a uniform bound with respect to the wavenumber κ, is given in the case of low frequency. The estimate provides a theoretical basis of the linearization algorithm. Properties on continuity and Fréchet differentiability of the scattering map are also examined. For analysis of the direct scattering in open domain, the reader is referred to [1, 8] and references therein. The relative permittivity or the scatterer is assumed to be constant with a known value inside inhomogeneities. The inverse obstacle scattering is to determine the number, shapes, sizes and locations of these inhomogeneities from the measurements of near field current densities, $\psi|_S$, given the incident field.

Our goal of this work is to present a recursive linearization method that solves the inverse obstacle scattering problem of Helmholtz equation in two dimensions. The reader is referred to [2, 6] and [3, 4] for recursive linearization approaches for solving inverse medium scattering problems in two dimensions and three dimensions, respectively. The algorithm requires multi-frequency scattering data, and the recursive linearization is obtained by a continuation method on the wavenumber κ. It first solves a linear equation (Born approximation) at the lowest κ, which maybe done by using the Fast Fourier Transform (FFT). Updates are subsequently obtained by using higher and higher wavenumber κ from the level set representation. Using the idea of Kaczmarz method [10, 11, 22, 23], we use partial data to perform the nonlinear Landweber iteration at each stage of the wavenumber κ. For each iteration, one forward and one adjoint state of the Helmholtz equation are solved.

The level set method was originally developed for describing the motion of curves and surfaces [25]. Since then, it has found application in a variety of quite different situations [24, 26]. The idea of using level set representation as part of a solution scheme for inverse problems involving obstacles can be found in [5, 11, 15, 21, 27]. For related results on the inverse obstacle problem, the reader is referred to [7, 9, 14, 18–20] and references therein. See [8] for an account of the recent progress on the general inverse scattering problem.

The plan of this paper is as follows. The analysis of the variational problem for direct scattering is presented in Section 2. The well-posedness of the direct scattering is proved, and important energy estimate is given, and the Fréchet differentiability of the scattering map is examined. Section 3 is devoted to the numerical study of the inverse obstacle scattering, and a regularized iterative linearization algorithm is proposed. Numerical examples are presented in Section 4. The paper is concluded with some remarks and directions for future research in Section 5.

2 Analysis of the scattering map

For convenience, denote the inner products

$$(u, v) = \int_B u \cdot \bar{v}, \quad \text{and} \quad \langle u, v \rangle = \int_S u \cdot \bar{v},$$

where the bar denotes the complex conjugate.

To state our boundary value problem, we introduce the bilinear form $a : H^1(B) \times H^1(B) \to \mathbb{C}$

$$a(u, v) = (\nabla u, \nabla v) - \kappa^2(\varepsilon u, v) - \mathrm{i}\kappa\langle u, v \rangle,$$

and the linear functional on $H^1(B)$

$$b(v) = \kappa^2(q\psi^{\mathrm{inc}}, v).$$

Then, we have the weak form of the boundary value problem (1.4) and (1.5): Find $\psi \in H^1(B)$ such that

$$a(\psi, \xi) = b(\xi), \quad \text{for all } \xi \in H^1(B). \tag{2.1}$$

Throughout the paper, C stands for a positive generic constant whose value may change step by step, but should be always be clear from the contexts.

Lemma 2.1. *Given the scatterer $q \in L^\infty(B)$, the direct scattering problem* (1.4)–(1.5) *has at most one solution.*

Proof. It suffices to show that $\psi = 0$ in B if $\psi^i = 0$ (no source term). From the Green's formula

$$0 = \int_B (\psi\Delta\bar{\psi} - \bar{\psi}\Delta\psi) = \int_S \left(\psi\partial_{\mathbf{n}}\bar{\psi} - \bar{\psi}\partial_{\mathbf{n}}\psi\right) = -2\mathrm{i}\kappa \int_S |\psi|^2,$$

we get $\psi = 0$ on S. The absorbing boundary condition on S yields further that $\partial_{\mathbf{n}}\psi = 0$ on S. By the Holmgren uniqueness theorem, $\psi = 0$ in $\mathbb{R}^2 \setminus B$. A unique continuation result [17] concludes that $\psi = 0$ in B.

□

Theorem 2.1. *If the wavenumber k is sufficiently small, the variational problem* (2.1) *admits a unique weak solution in $H^1(B)$. Furthermore, it holds the estimate*

$$\| \psi \|_{H^1(B)} \leq C\kappa \| q \|_{L^\infty(B)} \| \psi^{\mathrm{inc}} \|_{L^2(B)}, \tag{2.2}$$

where the constant C is independent of the wavenumber κ.

Proof. Decompose the bilinear form a into $a = a_1 + \kappa^2 a_2$, where

$$\begin{aligned} a_1(\psi, \xi) &= (\nabla\psi, \nabla\xi) - \mathrm{i}\kappa\langle\psi, \xi\rangle, \\ a_2(\psi, \xi) &= -(\varepsilon\psi, \xi). \end{aligned}$$

We conclude that a_1 is coercive from

$$\begin{aligned}|a_1(\psi,\psi)| &\geq C\left(\| \nabla\psi \|_{L^2(B)}^2 + \kappa \| \psi \|_{L^2(S)}^2\right)\\ &\geq C\kappa \| \psi \|_{H^1(B)}^2, \quad \text{for all } \psi \in H^1(B),\end{aligned}$$

where the last inequality may be obtained by applying standard elliptic estimates [13].

Next we prove the compactness of a_2. Define the operator $\mathcal{K} : L^2(B) \to H^1(B)$ by

$$a_1(\mathcal{K}\psi, \xi) = a_2(\psi, \xi), \quad \text{for all } \xi \in H^1(B),$$

which gives

$$(\nabla\mathcal{K}\psi, \nabla\xi) - \mathrm{i}\kappa\langle\mathcal{K}\psi, \xi\rangle = -(\varepsilon\psi, \xi), \quad \text{for all } \xi \in H^1(B).$$

Using the Lax–Milgram lemma, it follows that

$$\| \mathcal{K}\psi \|_{H^1(B)} \leq C\kappa^{-1} \| \psi \|_{L^2(B)}, \tag{2.3}$$

where the constant C is independent of k. Thus $\mathcal{K}$ is bounded from $L^2(B)$ to $H^1(B)$, and $H^1(B)$ is compactly imbedded into $L^2(B)$. Hence $\mathcal{K} : L^2(B) \to L^2(B)$ is a compact operator.

Define a function $u \in L^2(B)$ by requiring $u \in H^1(B)$ and satisfying

$$a_1(u, \xi) = b(\xi), \quad \text{for all } \xi \in H^1(B).$$

It follows from the Lax–Milgram lemma again that

$$\| u \|_{H^1(B)} \leq C\kappa \| q \|_{L^\infty(B)} \| \psi^{\mathrm{inc}} \|_{L^2(B)}. \tag{2.4}$$

Using the operator $\mathcal{K}$, we can see that the problem (2.1) is equivalent to find $\psi \in L^2(B)$ such that

$$(\mathcal{I} + \kappa^2\mathcal{A})\psi = u. \tag{2.5}$$

When κ is sufficiently small, the operator $\mathcal{I} + \kappa^2\mathcal{K}$ has a uniformly bounded inverse. We then have the estimate

$$\| \psi \|_{L^2(B)} \leq C \| u \|_{L^2(B)}, \tag{2.6}$$

where the constant C is independent of κ.

Rearranging (2.5), we have $\psi = u - \kappa^2\mathcal{K}\psi$, so $\psi \in H^1(B)$ and, by the estimate (2.3) for the operator $\mathcal{K}$, we have

$$\| \psi \|_{H^1(B)} \leq \| u \|_{H^1(B)} + C\kappa \| \psi \|_{L^2(B)}.$$

The proof is completed by combining (2.6) and (2.4).

□

Remark 2.1. *The energy estimate of the scattered field* (2.2) *provides a criterion for weak scattering. From this estimate, it is easily seen that fixing any two of the three quantities, i.e., the wavenumber κ, the compact support of the scatterer Ω, and the $L^\infty(B)$ norm of the scatterer, the scattering is weak when the third one is small. Especially, for the given scatterer $q(\mathbf{x})$, i.e., the norm and the compact support are fixed, the scattering is weak when the wavenumber κ is small.*

Remark 2.2. *For a general wavenumber κ, from the equation* (2.5)*, the existence follows from the Fredholm alternative and the uniqueness result. However, the constant C in the estimate* (2.2) *depends on the wavenumber.*

For a given scatterer q and an incident field ψ^{inc}, we define the map $S(q, \psi^{\text{inc}})$ by $\psi = S(q, \psi^{\text{inc}})$, where ψ is the solution of the problem (1.4)–(1.5) or the variational problem (2.1). It is easily seen that the map $S(q, \psi^{\text{inc}})$ is linear with respect to the incident field ψ^{inc} but is nonlinear with respect to q. Hence, we may denote $S(q, \psi^{\text{inc}})$ by $S(q)\psi^{\text{inc}}$.

Concerning the map $S(q)$, we have the following regularity results. Corollary 2.1 gives the boundedness of $S(q)$ and directly follows from Theorem 2.1; while a continuity result for the map $S(q)$ is presented in Lemma 2.2.

Corollary 2.1. *Given $q \in L^\infty(B)$, the scattering map $S(q)$ is a bounded linear map from $L^2(B)$ to $H^1(B)$. Moreover, there is a constant C depending on κ and B such that*

$$\| S(q)\psi^{\text{inc}} \|_{H^1(B)} \leq C \| q \|_{L^\infty(B)} \| \psi^{\text{inc}} \|_{L^2(B)} . \tag{2.7}$$

Lemma 2.2. *Assume that $q_1, q_2 \in L^\infty(B)$. Then*

$$\| (S(q_1) - S(q_2))\, \psi^{\text{inc}} \|_{H^1(B)} \leq C \| q_1 - q_2 \|_{L^\infty(B)} \| \psi^{\text{inc}} \|_{L^2(B)}, \tag{2.8}$$

where the constant C depends on $\kappa, B,$ and the bound of q_2.

Proof. Let $\psi_1 = S(q_1)\psi^{\text{inc}}$ and $\psi_2 = S(q_2)\psi^{\text{inc}}$. It follows that for $j = 1, 2$

$$\Delta\psi_j + \kappa^2(1 + q_j)\psi_j = -k^2 q_j \psi^{\text{inc}}.$$

By setting $w = \psi_1 - \psi_2$, we have

$$\Delta w + \kappa^2(1 + q_1)w = -\kappa^2(q_1 - q_2)(\psi^{\text{inc}} + \psi_2).$$

The function w also satisfies the boundary condition (1.5).

We repeat the procedure in the proof of Theorem 2.1 to obtain

$$\| w \|_{H^1(B)} \leq C \| q_1 - q_2 \|_{L^\infty(B)} \| \psi^{\text{inc}} + \psi_2 \|_{L^2(B)} .$$

Using Corollary 2.1 for ψ_2 yields

$$\| \psi_2 \|_{H^1(B)} \leq C \| q_2 \|_{L^\infty(B)} \| \psi^{\text{inc}} \|_{L^2(B)},$$

which gives

$$\| (S(q_1) - S(q_2))\, \psi^{\text{inc}} \|_{H^1(B)} \leq C \| q_1 - q_2 \|_{L^\infty(B)} \| \psi^{\text{inc}} \|_{L^2(B)},$$

where the constant C depends on $B, \kappa,$ and the bound of q_2.

□

Let γ be the restriction (trace) operator to the boundary S. By the trace theorem, γ is a bounded linear operator from $H^1(B)$ onto $H^{1/2}(S)$. We can now define the scattering map $M(q) = \gamma S(q)$. Next is to consider the Fréchet differentiability of the scattering map.

Recall the map $S(q)$ is nonlinear with respect to q. Formally, by using the first order perturbation theory, we obtain the linearized scattering problem of (1.4)–(1.5) with respect to a reference scatterer q,

$$\Delta v + \kappa^2(1 + q)v = -\kappa^2 \delta q(\psi^{\text{inc}} + \psi), \quad \text{in } \Omega, \tag{2.9}$$

$$\partial_{\mathbf{n}}\psi - \mathrm{i}\kappa v = 0, \quad \text{on } S, \tag{2.10}$$

where $\psi = S(q)\psi^{\text{inc}}$.

Define the formal linearization $T(q)$ of the map $S(q)$ by $v = T(q)(\delta q, \psi^{\text{inc}})$, where v is the solution of the problem (2.9)–(2.10). The following result is concerned with the boundedness for the map $T(q)$. A proof by be given by following step by step the proofs of Theorem 2.1 and Lemma 2.2. Hence we omit here.

Lemma 2.3. *Assume that $q, \delta q \in L^\infty(B)$, and $\psi^{\rm inc}$ is the incident field. Then $v = T(q)(\delta q, \psi^{\rm inc}) \in H^1(B)$ with the estimate*

$$\| T(q)(\delta q, \psi^{\rm inc}) \|_{H^1(B)} \leq C \| \delta q \|_{L^\infty(B)} \| \psi^{\rm inc} \|_{L^2(B)}, \tag{2.11}$$

where the constant C depends on κ, B, and q.

The next lemma is concerned with the continuity property of the map.

Lemma 2.4. *For any $q_1, q_2 \in L^\infty(B)$, and an incident field $\psi^{\rm inc}$, the following estimate holds*

$$\| T(q_1)(\delta q, \psi^{\rm inc}) - T(q_2)(\delta q, \psi^{\rm inc}) \|_{H^1(B)} \leq C \| q_1 - q_2 \|_{L^\infty(B)} \| \delta q \|_{L^\infty(B)} \| \psi^{\rm inc} \|_{L^2(B)}, \tag{2.12}$$

where the constant C depends on κ and B.

Proof. Let $v_i = T(q_i)(\delta q, \psi^{\rm inc})$, for $i = 1, 2$. It is easy to see that

$$\begin{aligned} \Delta(v_1 - v_2) + \kappa^2(1 + q_1)(v_1 - v_2) = \\ - \kappa^2 \delta q(\psi_1 - \psi_2) - \kappa^2(q_1 - q_2)v_2, \end{aligned}$$

where $\psi_i = S(q_i)\psi^{\rm inc}$.

Similar to the proof of Theorem 2.1, we get

$$\| v_1 - v_2 \|_{H^1(B)} \leq C \left(\| \delta q \|_{L^\infty(B)} \| \psi_1 - \psi_2 \|_{H^1(B)} + \| q_1 - q_2 \|_{L^\infty(B)} \| v_2 \|_{H^1(B)} \right)$$

From Corollary 2.1 and Lemma 2.2, we obtain

$$\| v_1 - v_2 \|_{H^1(B)} \leq C \| q_1 - q_2 \|_{L^\infty(B)} \| \delta q \|_{L^\infty(B)} \| \psi^{\rm inc} \|_{L^2(B)},$$

which completes the proof. □

The following result concerns the differentiability property of $S(q)$.

Lemma 2.5. *Assume that $q, \delta q \in L^\infty(B)$. Then there is a constant C dependent of κ and B, for which the following estimate holds*

$$\| S(q + \delta q)\psi^{\rm inc} - S(q)\psi^{\rm inc} - T(q)(\delta q, \psi^{\rm inc}) \|_{H^1(B)} \leq C \| \delta q \|^2_{L^\infty(B)} \| \psi^{\rm inc} \|_{L^2(B)} . \tag{2.13}$$

Proof. By setting $\psi_1 = S(q)\psi^{\rm inc}, \psi_2 = S(q + \delta q)\psi^{\rm inc}$, and $v = T(q)(\delta q, \psi^{\rm inc})$, we have

$$\begin{aligned} \Delta\psi_1 + \kappa^2(1 + q)\psi_1 &= -\kappa^2 q\psi^{\rm inc}, \\ \Delta\psi_2 + \kappa^2(1 + q + \delta q)\psi_2 &= -\kappa^2(q + \delta q)\psi^{\rm inc}, \\ \Delta v + \kappa^2(1 + q)v &= -\kappa^2\delta q\psi_1 - \kappa^2\delta q\psi^{\rm inc}. \end{aligned}$$

In addition, ψ_1, ψ_2, and v satisfy the absorbing boundary condition (1.5).

Denote $U = \psi_2 - \psi_1 - v$. Then

$$\Delta U + \kappa^2(1 + q)U = -\kappa^2\delta q(\psi_2 - \psi_1).$$

Similar arguments as in the proof of Lemma 2.1 gives

$$\| U \|_{H^1(B)} \leq C \| \delta q \|_{L^\infty(B)} \| \psi_2 - \psi_1 \|_{H^1(B)} .$$

From Lemma 2.1, we obtain further that

$$\| U \|_{H^1(B)} \leq C \| \delta q \|^2_{L^\infty(B)} \| \psi^{\rm inc} \|_{L^2(B)},$$

which is the estimate. □

Finally, by combining the above lemmas, we arrive at

Theorem 2.2. *The scattering map $M(q)$ is Fréchet differentiable with respect to q and its Fréchet derivative is*

$$DM(q) = \gamma T(q). \tag{2.14}$$

3 Inverse medium scattering

In this section, a regularized recursive linearization method for solving the inverse obstacle scattering problem of Helmholtz equation in two dimensions is proposed. The algorithm, obtained by a continuation method on the wavenumber κ, requires multi-frequency scattering data. At each wavenumber κ, the algorithm determines a forward model which produces the prescribed scattering data. At low wavenumber κ, the scattered field is weak. Consequently, the nonlinear equation become essentially a linear one, known as the Born approximation. The algorithm first solves this nearly linear equation at the lowest κ to obtain low-frequency modes of the true scatterer. The approximation is then used to linearize the nonlinear equation at the next higher κ to produce a better approximation which contains more modes of the true scatterer. This process is continued until a sufficiently high wavenumber κ where the dominant modes of the scatterer are essentially recovered. At each update, a level set representation is used to keep track of shapes of the scatterer.

3.1 shape reconstruction

We formulate the inverse obstacle scattering as shape reconstruction problem, and cast it in a form which makes use of the level set representation of the domains. To start with we introduce some useful notations.

Definition 3.1. *Assume that we are given a constant $\tilde{q} > 0$ and an open ball $B \subset \mathbb{R}^2$. We call a pair (Ω, q), which consists of a compact domain $\Omega \subset\subset B$ and $q \in L^\infty(B)$, admissible if we have*

$$q(\mathbf{x}) = \begin{cases} \tilde{q}, & \text{if } \mathbf{x} \in \Omega, \\ 0, & \text{if } \mathbf{x} \in \mathbb{R}^2 \setminus \Omega. \end{cases}$$

In other words, a pair (Ω, q) is admissible if q has a compact support of Ω with preassigned value $\tilde{q}$ inside. For an admissible pair (Ω, q), and for given $\tilde{q}$, the scatterer q is uniquely determined by Ω.

It is essential for the success and efficiency of the inverse obstacle scattering to have a good and flexible way of keeping track of the shape evolution during the reconstruction process. The method chosen in our reconstruction algorithm is a level set representation of the shapes [27].

Definition 3.2. *A function $\phi : \mathbb{R}^2 \to \mathbb{R}$ is called a level set representation of Ω if*

$$\phi|_\Omega \le 0 \quad \text{and} \quad \phi|_{\mathbb{R}^2 \setminus \Omega} > 0. \tag{3.1}$$

For each function $\phi : \mathbb{R}^2 \to \mathbb{R}$ there is a domain Ω associated with ϕ by (3.1) which is called scattering domain and denoted as $\Omega[\phi]$. It is clear that different functions $\phi_1, \phi_2, \phi_1 \ne \phi_2$, can be associated with the same domain $\Omega[\phi_1] = \Omega[\phi_2]$, but different domains cannot have the same level set representation. Therefore, we can use the level set representation for specifying a domain Ω by any one of its associated level set functions. The boundary of a domain $\Omega[\phi]$, represented by the level set function ϕ, is denoted $\Gamma = \partial\Omega[\phi]$.

Definition 3.3. *We call a triple (Ω, q, ϕ), which consists of a domain $\Omega \subset\subset B$ and $q, \phi \in L^\infty(B)$, admissible if the pair (Ω, q) is admissible in the sense of Definition 3.1, and ϕ is a level set representation of Ω.*

For an admissible triple (Ω, q, ϕ), and for given $\tilde{q}$, the pair (Ω, q) is uniquely determined by ϕ. The shape of the scatterer is then recovered from the representing level set function. We use these definitions to reformulate our inverse obstacle scattering problem: Given a constant $\tilde{q}$ and boundary measurements of the scattered field $\psi|_S$. Find a level set function ϕ such that the corresponding admissible triple (Ω, q, ϕ) reproduces the data.

A continuation method is proposed to recursively determine the triple (Ω_k, q_k, ϕ_k) at $k = \kappa_1, \kappa_2, ...$ with increasing wavenumber. For finding this series, we only need keep track of ϕ_k and q_k, but not of Ω_k. The function q_k is need in each step for solving a forward and a corresponding adjoint problem. The final level set function is used to recover the final shape of the scatterer.

3.2 Born approximation

For starting the shape reconstruction method, an initial guess is needed which is derived from the Born approximation. Rewrite (1.4) as

$$\Delta\psi + \kappa^2\psi = -\kappa^2 q(\psi^{\text{inc}} + \psi), \tag{3.2}$$

where the incident wave is taken as $\psi^{\text{inc}} = e^{\mathrm{i}\kappa\mathbf{x}\cdot\mathbf{d}_1}$. Consider a test function $\psi_0 = e^{\mathrm{i}\kappa\mathbf{x}\cdot\mathbf{d}_2}$, where $\mathbf{d}_2 \in \mathbb{S}^1$. Hence ψ_0 satisfies (1.3).

Multiplying (3.2) by ψ_0, and integrating over B on both sides, we have

$$\int_B \psi_0\Delta\psi + \kappa^2\int_B \psi_0\psi = -\kappa^2\int_B q(\psi^{\text{inc}} + \psi)\psi_0.$$

Integration by parts yields

$$\int_B \psi\Delta\psi_0 + \int_S \left(\psi_0\partial_{\mathbf{n}}\psi - \psi\partial_{\mathbf{n}}\psi_0\right) + \kappa^2\int_B \psi_0\psi = -\kappa^2\int_B q(\psi^{\text{inc}} + \psi)\psi_0.$$

We have by noting (1.3) and the boundary condition (1.5)

$$\int_B q(\psi^{\text{inc}} + \psi)\psi_0 = \frac{1}{\kappa^2}\int_S \psi\left(\partial_{\mathbf{n}}\psi_0 + \mathrm{i}\kappa\psi_0\right).$$

Using the special form of the incident wave and the test function, we then get

$$\int_B q(\mathbf{x})e^{\mathrm{i}\kappa\mathbf{x}\cdot(\mathbf{d}_1+\mathbf{d}_2)} = \mathrm{i}\kappa^{-1}\int_S \psi(\mathbf{n}\cdot\mathbf{d}_2 + 1)e^{\mathrm{i}\kappa\mathbf{x}\cdot\mathbf{d}_2} - \int_B q\psi\psi_0. \tag{3.3}$$

From Theorem 2.1, for small wavenumber κ, the scattered field is weak and the inverse scattering problem becomes essentially linear. Dropping the nonlinear (second) term of the equation (3.3), we obtain the linearized integral equation

$$\int_B q(\mathbf{x})e^{\mathrm{i}\kappa\mathbf{x}\cdot(\mathbf{d}_1+\mathbf{d}_2)} = \mathrm{i}\kappa^{-1}\int_S \psi(\mathbf{n}\cdot\mathbf{d}_2 + 1)e^{\mathrm{i}\kappa\mathbf{x}\cdot\mathbf{d}_2}, \tag{3.4}$$

which is the Born approximation.

Since the scatterer $q(\mathbf{x})$ has a compact support, we use the notation

$$\hat{q}(\boldsymbol{\xi}) = \int_B q(\mathbf{x}) e^{\mathrm{i}\kappa \mathbf{x}\cdot(\mathbf{d}_1+\mathbf{d}_2)},$$

where $\hat{q}(\boldsymbol{\xi})$ is the Fourier transform of $q(\mathbf{x})$ with $\boldsymbol{\xi} = \kappa(\mathbf{d}_1 + \mathbf{d}_2)$. Choose

$$\mathbf{d}_j = (\cos\theta_j, \sin\theta_j), \quad j = 1, 2,$$

where θ_j is the incident angle. It is obvious that the domain $[0, 2\pi]$ of $\theta_j, j = 1, 2$, corresponds to the ball $\{\boldsymbol{\xi} : |\boldsymbol{\xi}| \le 2\kappa\}$. Thus, the Fourier modes of $\hat{q}(\boldsymbol{\xi})$ in the ball $\{\boldsymbol{\xi} : |\boldsymbol{\xi}| \le 2k\}$ can be determined. The scattering data with the higher wavenumber κ must be used in order to recover more modes of the true scatterer.

Define the data

$$G(\boldsymbol{\xi}) = \begin{cases} \mathrm{i}\kappa^{-1} \int_S \psi(\mathbf{n}\cdot\mathbf{d}_2 + 1) e^{\mathrm{i}\kappa\mathbf{x}\cdot\mathbf{d}_2}, & \text{for } |\boldsymbol{\xi}| \le 2\kappa, \\ 0, & \text{otherwise.} \end{cases}$$

The linear integral equation (3.4) can be reformulated as

$$\int_{\mathbb{R}^2} q(\mathbf{x}) e^{\mathrm{i}\mathbf{x}\cdot\boldsymbol{\xi}} d\mathbf{x} = G(\boldsymbol{\xi}). \tag{3.5}$$

Taking the inverse Fourier transform of the equation (3.5) leads to

$$(2\pi)^{-2} \int_{\mathbb{R}^2} e^{-\mathrm{i}\mathbf{x}\cdot\boldsymbol{\xi}} \big[\int_{\mathbb{R}^2} q(\mathbf{y}) e^{\mathrm{i}\mathbf{y}\cdot\boldsymbol{\xi}} d\mathbf{y}\big] d\boldsymbol{\xi} = (2\pi)^{-2} \int_{\mathbb{R}^2} e^{-\mathrm{i}\mathbf{x}\cdot\boldsymbol{\xi}} G(\boldsymbol{\xi}) d\boldsymbol{\xi}.$$

By the Fubini theorem, we have

$$(2\pi)^{-2} \int_{\mathbb{R}^2} q(\mathbf{y}) \big[\int_{\mathbb{R}^2} e^{\mathrm{i}(\mathbf{y}-\mathbf{x})\cdot\boldsymbol{\xi}} d\boldsymbol{\xi}\big] d\mathbf{y} = (2\pi)^{-2} \int_{\mathbb{R}^2} e^{-\mathrm{i}\mathbf{x}\cdot\boldsymbol{\xi}} G(\boldsymbol{\xi}) d\boldsymbol{\xi}.$$

Using the inverse Fourier transform of the Dirac Delta function

$$(2\pi)^{-2} \int_{\mathbb{R}^2} e^{\mathrm{i}(\mathbf{y}-\mathbf{x})\cdot\boldsymbol{\xi}} d\boldsymbol{\xi} = \delta(\mathbf{y} - \mathbf{x}),$$

we deduce

$$\int_{\mathbb{R}^2} q(\mathbf{y}) \delta(\mathbf{y} - \mathbf{x}) d\mathbf{y} = (2\pi)^{-2} \int_{\mathbb{R}^2} e^{-\mathrm{i}\mathbf{x}\cdot\boldsymbol{\xi}} G(\boldsymbol{\xi}) d\boldsymbol{\xi},$$

which gives

$$q(\mathbf{x}) = (2\pi)^{-2} \int_{\mathbb{R}^2} e^{-\mathrm{i}\mathbf{x}\cdot\boldsymbol{\xi}} G(\boldsymbol{\xi}) d\boldsymbol{\xi}. \tag{3.6}$$

In practice, the integral equation (3.6) is implemented by using the Fast Fourier Transform (FFT). We are now ready to define the initial triple (Ω, q, ϕ).

Choose a threshold value $0 < \tau < 1$ and define

$$q_0 := \tau \max_{\mathbf{x}\in B} |q(\mathbf{x})|.$$

The level set zero of ϕ is denoted as $\{\mathbf{x} \in B : |q(\mathbf{x})| = q_0\}$. This means that all points of B where the reconstruction $|q(\mathbf{x})|$ has exactly the value q_0 are mapped to zero by the level set function ϕ. The level set function is then defined as

$$\phi(\mathbf{x}) = \sigma(q_0 - |q(\mathbf{x})|),$$

where σ is some scaling factor. The initial scattering domain Ω and the scatterer are defined as

$$\Omega = \Omega[\phi], \quad q = \Lambda(\phi).$$

Together with ϕ they form an admissible triple (Ω, q, ϕ).

3.3 Recursive linearization

As discussed in the previous section, when the wavenumber κ is small, the Born approximation allows a reconstruction of those Fourier modes less than or equal to 2κ for the function $q(\mathbf{x})$. We now describe a procedure that recursively determines the triple (Ω_k, q_k, ϕ_k) at $k = k_j$ for $j = 1, 2, ...$ with the increasing wavenumber. At each stage of the wavenumber κ, using the idea of Kaczmarz method, we use partial data, corresponding to one incident wave, to perform the nonlinear Landweber iteration. Suppose now that the pair $(\Omega_{\tilde{k}}, q_{\tilde{k}})$ has been recovered at some wavenumber $\tilde{\kappa}$, and that $\kappa > 0$ is slightly larger than $\tilde{\kappa}$. Since only the ϕ_k and q_k need to be kept track, we wish to determine the ϕ_k and q_k, or equivalently, to determine the perturbation

$$\delta\phi = \phi_k - \phi_{\tilde{k}}, \quad \text{and} \quad \delta q = q_k - q_{\tilde{k}}.$$

For the reconstructed scatterer $q_{\tilde{k}}$, we solve at the wavenumber κ the forward scattering problem

$$\Delta\tilde{\psi} + \kappa^2(1 + q_{\tilde{k}})\tilde{\psi} = -\kappa^2 q_{\tilde{k}}\psi_j^{\mathrm{inc}}, \tag{3.7}$$

$$\partial_{\mathbf{n}}\tilde{\psi} - \mathrm{i}\kappa\tilde{\psi} = 0, \tag{3.8}$$

where ψ_j^{inc} is the incident wave with the incident angle $\theta_j = 2\pi j/J, j = 1, 2, ..., J$. For the scatterer q_k, we have

$$\Delta\psi + \kappa^2(1 + q_k)\psi = -\kappa^2 q_k\psi_j^{\mathrm{inc}}, \tag{3.9}$$

$$\partial_{\mathbf{n}}\psi - \mathrm{i}\kappa\psi = 0. \tag{3.10}$$

Subtracting (3.7), (3.8) from (3.9), (3.10) and omitting the second-order smallness in δq and in $\delta\psi = \psi - \tilde{\psi}$, we obtain

$$\Delta\delta\psi + \kappa^2(1 + q_{\tilde{k}})\delta\psi = -\kappa^2\delta q(\psi_j^{\mathrm{inc}} + \tilde{\psi}), \tag{3.11}$$

$$\partial_{\mathbf{n}}\psi - \mathrm{i}\kappa\delta\psi = 0. \tag{3.12}$$

For the scatterer q_k, and the incident wave ψ_j^{inc}, we define the map $S(q_k, \psi_j^{\mathrm{inc}})$ by

$$S(q_k, \psi_j^{\mathrm{inc}}) = \psi,$$

where ψ is the scattering data at the wavenumber k . Let γ be the trace operator to the boundary S. Define the scattering map

$$M(q_k, \psi_j^{\mathrm{inc}}) = \gamma S(q_k, \psi_j^{\mathrm{inc}}).$$

For simplicity, denote $M(q_k, \psi_j^{\mathrm{inc}})$ by $M_j(q_k)$. By the definition of the trace operator, we have

$$M_j(q_k) = \psi|_S.$$

Let $DM_j(q_{\tilde{k}})$ be the Fréchet derivative of $M_j(q_k)$, and denote the residual operator

$$R_j(q_{\tilde{k}}) = \psi|_S - \tilde{\psi}|_S.$$

It follows from Theorem 2.2 that

$$DM_j(q_{\tilde{k}})\delta q = R_j(q_{\tilde{k}}). \tag{3.13}$$

Given a constant $\tilde{q}$. Then, with each level set function ϕ a uniquely determined scatterer $\Lambda(\phi)$ is associated by putting

$$\Lambda(\phi)(x) = \begin{cases} \tilde{q}, & \text{for } \phi(x) \leq 0, \\ 0, & \text{for } \phi(x) > 0. \end{cases}$$

In [27], it is shown that the infinitesimal response δq in the scatterer $q(x)$ to an infinitesimal change $\delta\phi(x)$ of the level set function $\phi(x)$ has the form

$$\delta q(x) = -\tilde{q}\, \frac{\delta\phi(x)}{|\nabla\phi(x)|}\bigg|_{x\in\partial\Omega[\phi]}.$$

The Fréchet derivative of Λ is then defined [11]

$$[D\Lambda(\phi)\delta\phi](x) = -\tilde{q}\frac{\delta\phi(x)}{|\nabla\phi(x)|}\delta_\Gamma(x),$$

where $\delta_\Gamma(x)$ denotes the Dirac delta distribution concentrated on $\Gamma = \partial\Omega[\phi]$.

Define the forward operator

$$F_j(\phi) = M_j(\Lambda(\phi)) = \psi|_S, \tag{3.14}$$

where ψ is the scattered field with scatterer $\Lambda(\phi)$. It is easily seen that the Fréchet derivative of the forward operator can be expressed as

$$DF_j(\phi)\delta\phi = DM_j(\Lambda(\phi))D\Lambda(\phi)\delta\phi,$$

which gives by noting (3.13)

$$DF_j(\phi)\delta\phi = R_j(\Lambda(\phi)). \tag{3.15}$$

Using the Landweber iteration of (3.15) yields

$$\delta\phi = \beta_k DF_j^*(\phi)R(\Lambda(\phi)),$$

which gives

$$\delta\phi = \beta_k D\Lambda^*(\phi)DM_j^*(\Lambda(\phi))R_j(\Lambda(\phi)), \tag{3.16}$$

where β_k is a relaxation parameter.

In order to calculate (3.16), we will need practically useful expressions for the adjoint of the Fréchet derivatives. First, a simple calculation gives the following theorem.

Theorem 3.1. *The adjoint operator $D\Lambda^*(\phi)$ is given by*

$$\left[D\Lambda^*(\phi)\delta q\right](x) = -\tilde{q}\frac{\delta q}{|\nabla\phi|}\delta_\Gamma(x). \tag{3.17}$$

Theorem 3.2. *Given residual $R_j(q_{\tilde{k}})$, there exits a function φ_j such that the adjoint Fréchet derivative $DM_j^*(q_{\tilde{k}})$ satisfies*

$$\left[DM_j^*(q_{\tilde{k}})R_j(q_{\tilde{k}})\right](x) = k^2\big(\bar{\psi}_j^{\rm inc}(x) + \bar{\tilde{\psi}}(x)\big)\varphi_j(x), \tag{3.18}$$

where the bar denotes the complex conjugate, $\phi_j^{\rm inc}$ is the incident wave with incident angle θ_j, and $\tilde{\psi}_j$ is the solution of (3.7), (3.8) *with the incident wave $\psi_j^{\rm inc}$.*

Proof. Let $\tilde{\psi}_j$ be the solution of (3.7), (3.8) with the incident wave $\psi_j^{\rm inc}$. Consider the equations as follows

$$\Delta\delta\psi + \kappa^2(1+q_{\tilde{k}})\delta\psi = -\kappa^2\delta q(\psi_j^{\rm inc} + \tilde{\psi}), \tag{3.19}$$

$$\partial_{\mathbf{n}}\delta\psi - \mathrm{i}\kappa\delta\psi = 0. \tag{3.20}$$

and the adjoint equations

$$\Delta\varphi_j + \kappa^2(1+q_{\tilde{k}})\varphi_j = 0, \tag{3.21}$$
$$\partial_{\mathbf{n}}\varphi_j + \mathrm{i}\kappa\varphi_j = R_k(q_{\tilde{k}}). \tag{3.22}$$

The existence and uniqueness of the weak solution for the adjoint equations follow from the same proof of Corollary 2.1, we omit here.

Multiplying equation (3.19) with the complex conjugate of φ_j, integrating over B on both sides, we obtain

$$\int_B \bar{\varphi}_j \Delta\delta\psi + \kappa^2\int_B (1+q_{\tilde{k}})\delta\psi\bar{\varphi}_j = -\kappa^2\int_B \delta q\big(\psi_j^{\mathrm{inc}} + \tilde{\psi}\big)\bar{\varphi}_j.$$

Integration by parts yields

$$\int_S \big(\bar{\varphi}_j\partial_{\mathbf{n}}\delta\psi - \delta\psi\overline{\partial_{\mathbf{n}}\varphi_j}\big) = -\kappa^2\int_B \delta q\big(\psi_j^{\mathrm{inc}} + \tilde{\psi}\big)\bar{\varphi}_j.$$

Using the boundary condition (3.20), we deduce

$$\int_S \delta\psi\big(\overline{\partial_{\mathbf{n}}\varphi_j} - \mathrm{i}\kappa\bar{\varphi}_j\big) = \kappa^2\int_B \delta q\big(\psi_j^{\mathrm{inc}} + \tilde{\psi}\big)\bar{\varphi}_j dx$$

It follows from (3.13), and the boundary condition (3.22)

$$\int_S \big[DM_j(q_{\tilde{k}})\delta q\big]\overline{R_j(q_{\tilde{k}})} = \kappa^2\int_B \delta q\big(\psi_j^{\mathrm{inc}} + \tilde{\psi}\big)\bar{\varphi}_j$$

We know from the adjoint operator $DM_j^*(q_{\tilde{k}})$

$$\int_B \delta q\overline{DM_j^*(q_{\tilde{k}})R_j(q_{\tilde{k}})} = \kappa^2\int_B \delta q\big(\psi_j^{\mathrm{inc}} + \tilde{\psi}\big)\bar{\varphi}_j.$$

Since it holds for any δq, we have

$$\overline{DM_j^*(q_{\tilde{k}})R_j(q_{\tilde{k}})} = \kappa^2\big(\psi_j^{\mathrm{inc}} + \tilde{\psi}\big)\bar{\varphi}_j.$$

Taking the complex conjugate of the above equation yields the result.

□

Finally, combining Theorems 3.1 and 3.2, It follows that (3.16) can be rewritten as

$$\delta\phi = -\tilde{q}\kappa^2\beta_k\frac{(\bar{\psi}_j^{\mathrm{inc}} + \bar{\tilde{\psi}}_j)\varphi_j}{|\nabla\phi|}\delta_\Gamma(x). \tag{3.23}$$

In practice, for a given level set function ϕ, let $\Gamma = \partial\Omega[\phi]$ and $B_\rho(\Gamma) = \cup_{y\in\Gamma}B_\rho(y)$ a small finite width neighborhood of Γ. In our numerical experiment, the constant ρ is chosen about 2-3 grid cells. Equation (3.23) is updated with

$$\delta\phi = -\tilde{q}\kappa^2\beta_k\frac{(\bar{\psi}_j^{\mathrm{inc}} + \bar{\tilde{\psi}}_j)\varphi_j}{|\nabla\phi|}\chi_{B_\rho(\Gamma)}(x), \tag{3.24}$$

where β_k is some suitable parameter and $\chi_{B_\rho(\Gamma)}(x)$ is defined as

$$\chi_{B_\rho(\Gamma)}(x) = \begin{cases} 1, & \text{for } x \in B_\rho(\Gamma), \\ 0, & \text{for } \mathbb{R}^2 \setminus B_\rho(\Gamma). \end{cases}$$

Table 1: Recursive linearization reconstruction algorithm.

Initialization
$k = k_0$
$(\Omega_{k_0}, q_{k_0}, \phi_{k_0})$ given from the Born approximation
Reconstruction loop
  do $k = k_{\min} : k_{\max}$ march over wavenumber
    do $j = 1 : J$ perform J sweeps for incident angles
      $\delta\phi_{jk} = -\tilde{q}\kappa^2\beta_k \frac{(\bar{\psi}_j^{\mathrm{inc}}+\bar{\tilde{\psi}}_j)\varphi_j}{|\nabla\phi_{jk}|}\chi_{B_\rho(\Gamma)}$
      $\phi_{jk} := \phi_{jk} + \delta\phi_{jk}$
      $q_{jk} := \Lambda(\phi_{jk})$
    end do
    $\phi_k := \phi_{Jk}$
    $q_k := \Lambda(\phi_k)$
  end do
  $(\Omega, q, \phi) := (\Omega_{k_{\max}}, q_{k_{\max}}, \phi_{k_{\max}})$ final reconstruction

So for each incident wave with incident angel θ_j, we have to solve one forward problem (3.7), (3.8), and one adjoint problem (3.21), (3.22). Since the adjoint problem has a similar variational form with the forward problem. Essentially, we need to compute two forward problems at each sweep. Once $\delta\phi_j$ is determined, $\phi_{\tilde{\eta}}$ is updated by $\phi_{\tilde{k}} + \delta\phi_j$. After completing the Jth sweep, we get the reconstructed level set function ϕ_η at the spatial frequency η. Then, the scatterer is updated by $q_k = \Lambda(\phi_k)$.

Remark 3.1. *For a fixed wavenumber κ, the stopping index of nonlinear Landweber iteration* (3.16) *could be determined from the discrepancy principle. However, in practice, it is not necessary to do many iterations. Numerical results show that the iterative process for different incident angles $\phi_j, j = 1, ..., m$, is sufficient to obtain reasonable accuracy.*

The recursive linearization for shape reconstruction of inverse medium scattering can be summarized in Table 1.

4 Numerical experiments

In this section, we discuss the numerical solution of the forward scattering problem, and the computational issues of the recursive linearization algorithm.

As for the forward solver, we adopt the Finite Element Method (FEM). As we know, the FEM usually leads to a sparse matrix. The sparse large-scale linear system can be most efficiently solved if the zero elements of coefficient matrix are not stored. We used the commonly used Compressed Row Storage (CRS) format which makes no assumptions about the sparsity structure of the matrix, and does not store any unnecessary elements. In fact, from the variational formula of our direct problem (2.1), the coefficient matrix is complex symmetric. Hence, only the lower triangular portion of the matrix needs be stored. Regarding the linear solver, both BiConjugate Gradient (BiCG) and Quasi-Minimal Residual (QMR) algorithms with diagonal preconditioning are tried to solve the sparse, symmetric, and complex system of the equations, with the QMR more efficient.

In the following, we present three numerical examples where the number of incident wave $J = 10$ and the relaxation parameter $\beta_k = 0.1/\kappa$. For stability analysis, some relative random noise is added to the date, i.e., the electric field takes the form

$$\psi|_S := (1 + \sigma\,\mathrm{rand})\psi|_S.$$

Here, rand gives normally distributed random numbers in $[-1, 1]$, and σ is a noise level parameter, taken to be 0.02 in our numerical experiments.

Example 1. Reconstruct a U-shaped scatterer in the domain $D = [-1,\,1] \times [-1,\,1]$. Figure 1 shows the exact scatterer and the evolution of reconstructions at different wavenumbers varying from the Born approximation with wavenumber $\kappa = 1.0$ to highest wavenumber $\kappa = 7.0$. As can be seen, better reconstructions are obtained when higher wavenumber is used for the inversion. Under the lowest wavenumber, the Born approximation can only generate an average of the scatterer; no detailed features are able to be resolved. The concave part of the scatterer can be gradually resolved by using higher and higher wavenumbers; while the concave part of the scatterer can not be fully recovered at the low wavenumber. This result may be explained by Heisenberg's uncertainty principle [6]. We point out that the method is not sensitive to the noise and the step size of the wavenumber, which suggests that large step size of the wavenumber may be used to speed up the convergence. Figure 2 shows the negative of the level set function $-\phi$, which clearly presents the U shape of the reconstructed scatterer.

Example 2. Reconstruct a cross-shaped scatterer in the domain $D = [-1,\,1] \times [-1,\,1]$. Figure 3 shows the exact scatterer and the evolution of reconstructions at different wavenumbers varying from the Born approximation with wavenumber $\kappa = 1.0$ to highest wavenumber $\kappa = 7.0$. Similarly, better reconstructions are obtained when higher wavenumber is used for the inversion. Under the lowest wavenumber, the Born approximation can only generate an average of the scatterer; no detailed features are able to be resolved. The cross shape the scatterer can be gradually resolved by using higher and higher wavenumbers. Figure 4 shows the negative of the level set function $-\phi$, which clearly presents the cross shape of the reconstructed scatterer.

Example 3. Finally, we consider a scatterer which has three disjoint components. This scatterer is difficult to recover due to the three nearby components. Again, Figure 5 shows the exact scatterer and the evolution of reconstructions at different wavenumbers varying from the Born approximation with wavenumber $\kappa = 1.0$ to highest wavenumber $\kappa = 7.0$. Similarly, better reconstructions are obtained when higher wavenumber is used for the inversion and three components can be separated. Under the lowest wavenumber, the Born approximation can only generate an average of the scatterer; the three disjoint parts can not be resolved. The three parts of the scatterer can be gradually separated by using higher and higher wavenumbers. Figure 6 shows the negative of the level set function $-\phi$, which clearly presents the three parts of the reconstructed scatterer.

5 Concluding remarks

A new continuation method with respect to the spatial frequency of the evanescent plane waves is presented. The recursive linearization algorithm is robust and efficient for solving the inverse medium scattering with the fixed frequency scattering data. Finally, we point out two important future directions along the line of this work. The first is concerned with the convergence analysis. Although our numerical experiments demonstrate the convergence and stability of the inversion algorithm, its analysis needs to be done. Another important project is to consider the case of data with partial measurements at fixed frequency. Without the full measurements, the ill-posedness and nonlinearity of the inverse problem becomes more severe, which will be reported else where.

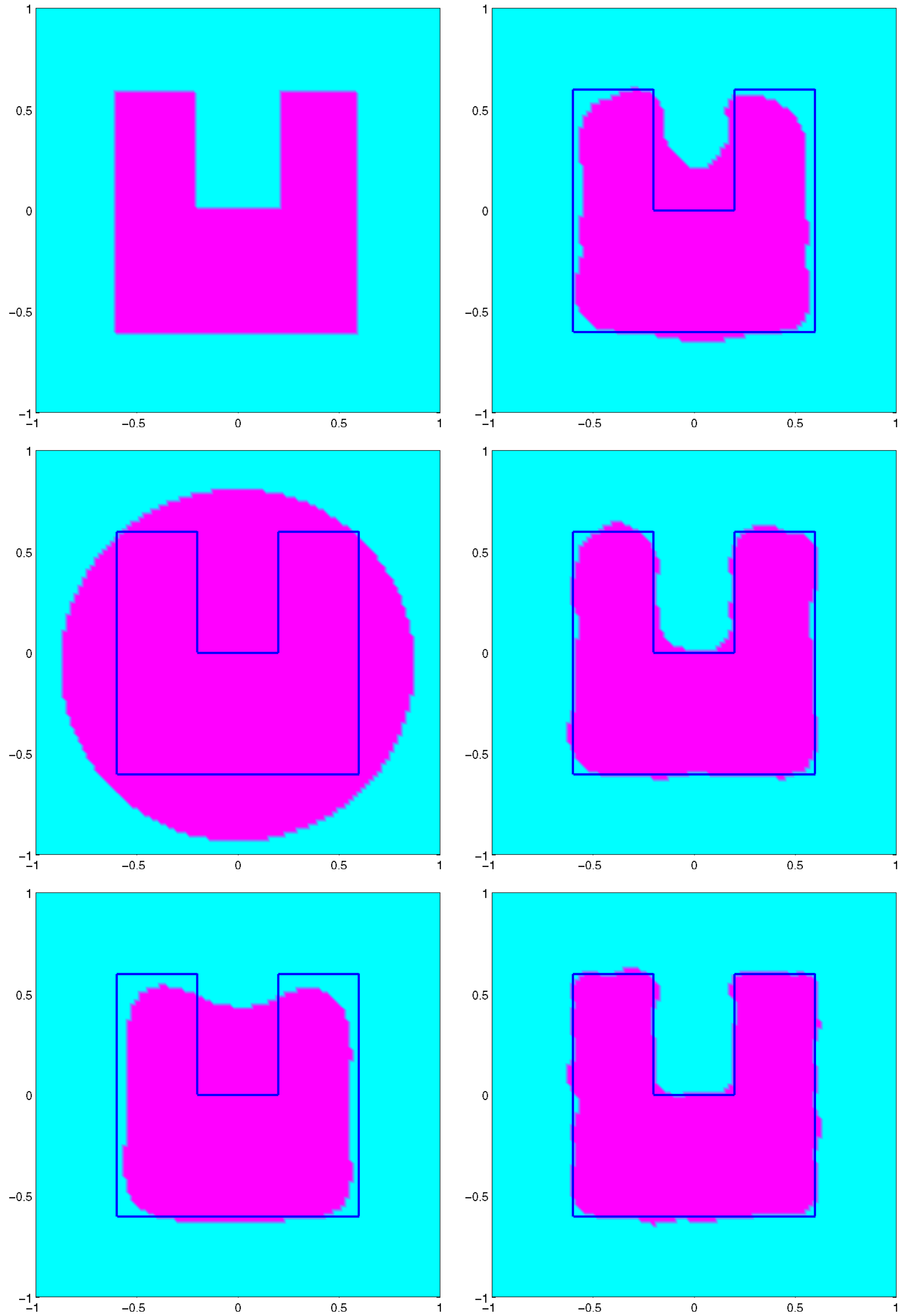

Figure 1: Evolution of scatterer in Example 1. Left column from top to bottom: true scatterer; Born approximation; reconstruction at $\kappa = 2.5$; right column from top to bottom: reconstruction at $\kappa = 4.0$; reconstruction at $\kappa = 5.5$; reconstruction at $\kappa = 7.0$..

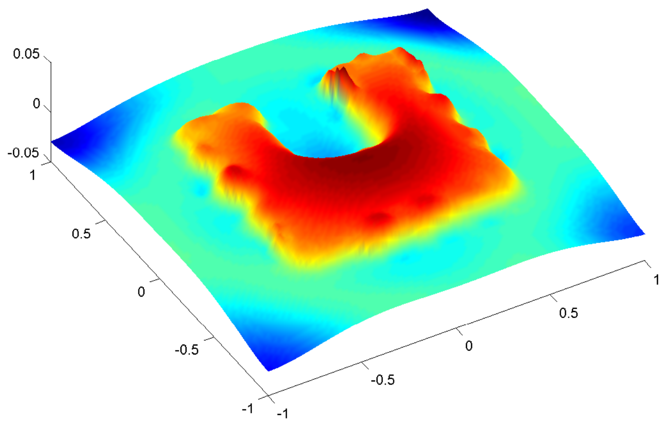

Figure 2: Final level set function $-\phi$ for Example 1.

References

[1] G. Bao, Y. Chen, and F. Ma, Regularity and stability for the scattering map of a linearized inverse medium problem, J. Math. Anal. Appl. , 247 (2000), 255–271.

[2] G. Bao and J. Liu, Numerical solution of inverse problems with multi-experimental limited aperture data, SIAM J. Sci. Comput., 25 (2003), 1102–1117.

[3] G. Bao and P. Li, Inverse medium scattering for three-dimensional time harmonic Maxwell equations, Inverse Problems, 20 (2004), L1–L7.

[4] G. Bao and P. Li, Inverse medium scattering problems for electromagnetic waves, SIAM J. Appl. Math., 65 (2005), 2049–2066.

[5] M. Burger, Levenberg-Marquardt level set methods for inverse obstacle problems, Inverse Problems, 20 (2004), 259–282.

[6] Y. Chen, Inverse scattering via Heisenberg uncertainty principle, Inverse Problems, 13 (1997), 253–282.

[7] D. Colton, H. Haddar, and M. Piana, The linear sampling method in inverse electromagnetic scattering theory, Inverse problems, 19 (2003), S105–S137.

[8] D. Colton and R. Kress, Inverse Acoustic and Electromagnetic Scattering Theory, 2nd ed., Appl. Math. Sci. 93, Springer-Verlag, Berlin, 1998.

[9] D. Colton and A. Kirsch, A simple method for solving inverse scattering problems in the resonance regions, Inverse Problems, 13 (1996), 383–393.

[10] O. Dorn, H. Bertete-Aguirre, J. G. Berryman, and G. C. Papanicolaou, A nonlinear inversion method for 3D electromagnetic imaging using adjoint fields, Inverse Problems, 15 (1999), 1523–1558.

[11] O. Dorn, E. Miller, and C. Rappaport, A shape reconstruction method for electromagnetic tomography using adjoint fields and level sets, Inverse Problems, 16 (2000), 1119–1156.

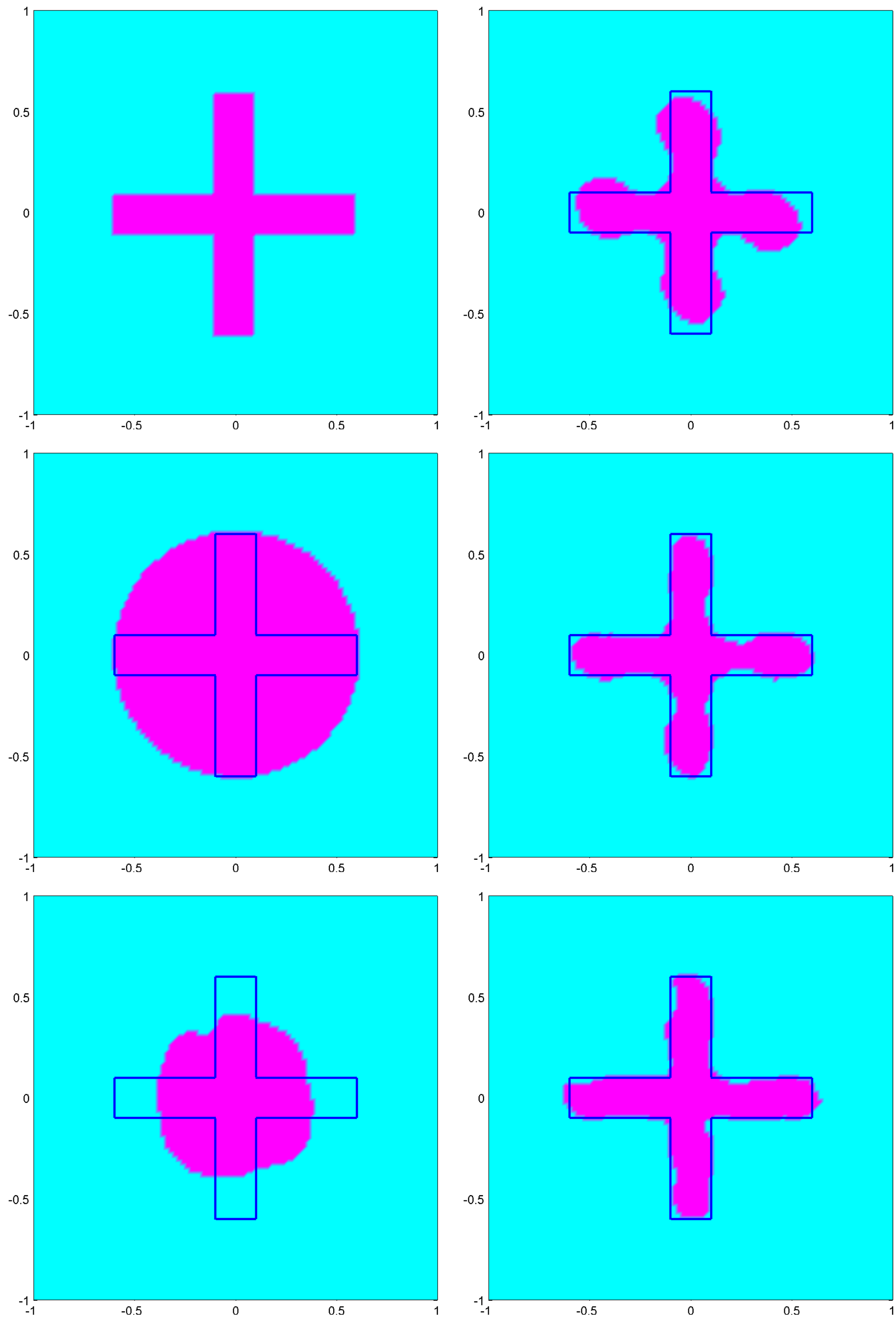

Figure 3: Evolution of scatterer in Example 2. Left column from top to bottom: true scatterer; Born approximation; reconstruction at $\kappa = 2.5$; right column from top to bottom: reconstruction at $\kappa = 4.0$; reconstruction at $\kappa = 5.5$; reconstruction at $\kappa = 7.0$.

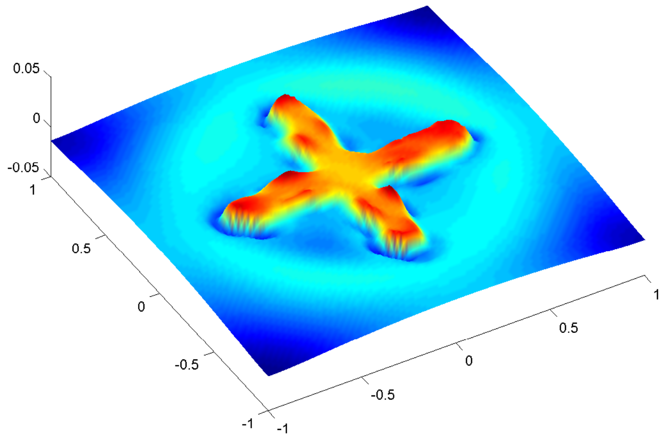

Figure 4: Final level set function $-\phi$ for Example 2.

[12] H. Engl, M. Hanke, and A. Neubauer, Regularization of Inverse Problems, Dordrecht: Kluwer, 1996.

[13] D. Gilbarg and N. Trudinger, Elliptic Partial Differential Equations of Second Order, New York: Springer, 1983.

[14] H. Haddar and P. Monk, The linear sampling method for solving the electromagnetic inverse medium problem, Inverse Problems, 18 (2002), 891–906.

[15] K. Ito, K. Kunisch, and Z. Li, Level-set function approach to an inverse interface problem, Inverse Problems, 17 (2001), 1225–1242.

[16] J. Jin, The finite element methods in Electromagnetics, John Wiley & Sons, 2002.

[17] D. Jerison and C. Kenig, Unique continuation and absence of positive eigenvalues for Schrödinger operators, Ann. Math., 121 (1985), 463–488.

[18] R. Kress, Decomposition methods in inverse obstacle scattering via Newton iterations, Proceedings of the 6th International Wrokshop on Mathematical Methods in Scattering Theory and Biomedical Engineering, Tsepelovo, 2003, to appear.

[19] R. Kress and W. Rundell, Inverse scattering for shape and impedance, Inverse Problems, 17 (2001), 1075–1085.

[20] R. Kress and W. Rundell, Inverse obstacle scattering using reduced data, SIAM J. Appl. Math., 59 (1999), 442–454.

[21] A. Litman, D. Lesselier, and F. Santosa, Reconstruction of a two-dimensional binary obstacle by controlled evolution of a level- set, Inverse Problems, 14 (1998), 685–706.

[22] F. Natterer, The Mathematics of Computerized Tomography, Stuttgart: Teubner, 1986.

[23] F. Natterer and F. Wübbeling, A propagation-backpropagation method for ultrasound tomography, Inverse Problems, 11 (1995), 1225–1232.

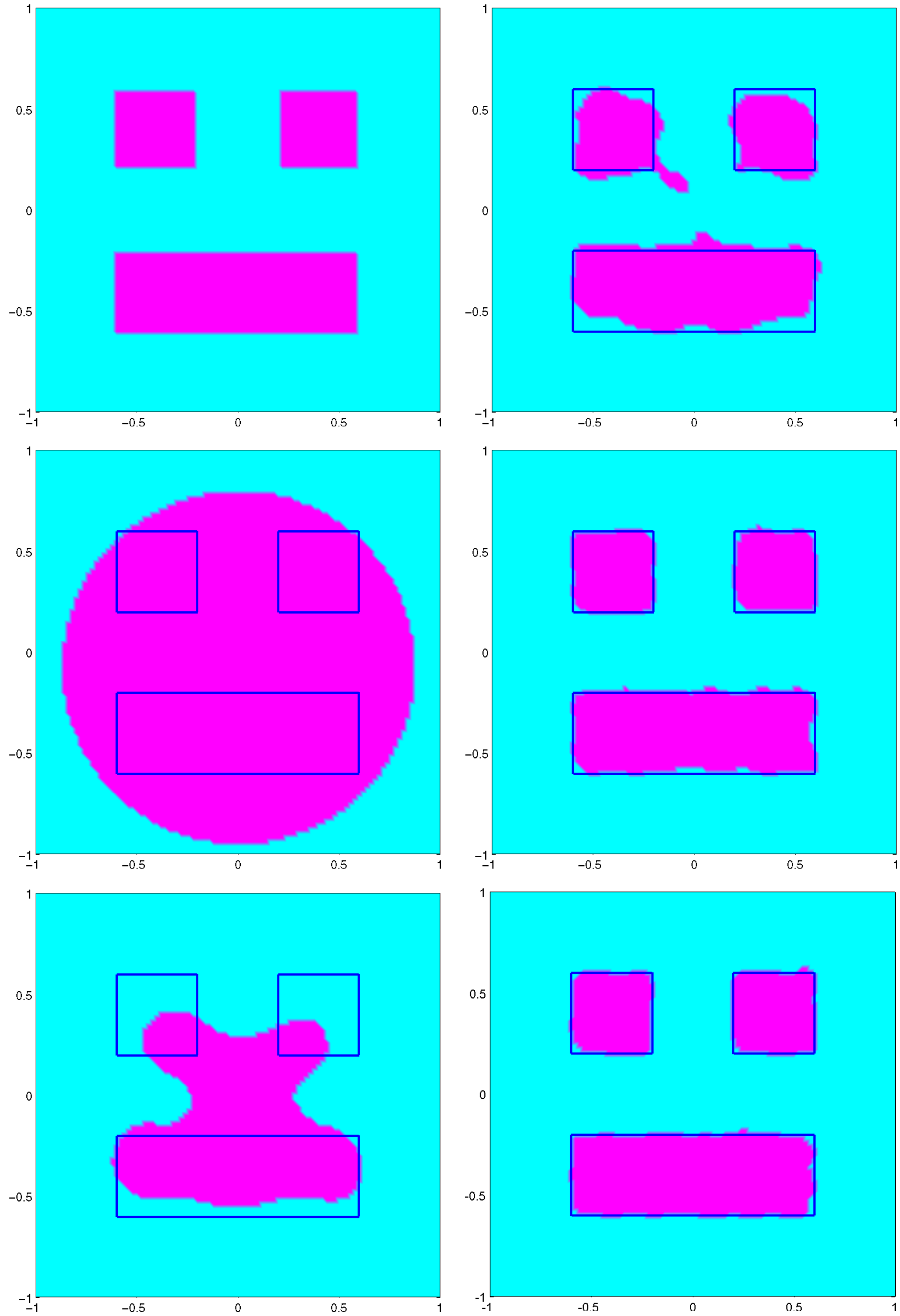

Figure 5: Evolution of scatterer in Example 3. Left column from top to bottom: true scatterer; Born approximation; reconstruction at $\kappa = 2.5$; right column from top to bottom: reconstruction at $\kappa = 4.0$; reconstruction at $\kappa = 5.5$; reconstruction at $\kappa = 7.0$.

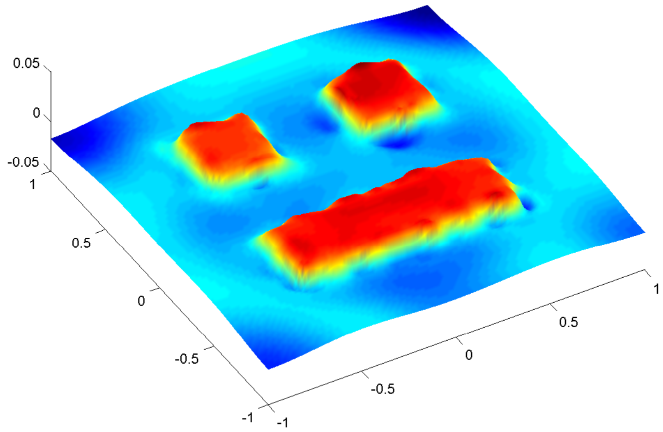

Figure 6: Final level set function $-\phi$ for Example 3.

[24] S. Osher and R. Fedkiw, Level set methods and dynamic implicit surfaces, New York: Springer, 2002.

[25] S. Osher and J. Sethian, Fronts propagating with curvature-dependent speed: algorithms based on Hamilton-Jacobi formulations, J. Comput. Phys., 79 (1988), 12–49.

[26] J. Sethian, Level set methods and fast marching methods, 2nd edn, Cambridge: Cambridge University Press, 1999.

[27] F. Santosa, A level-set approach for inverse problems involving obstacles, ESAIM: Control, Optimization and Calculus of Variations, 1 (1996), 17–33.